

Pharmacophore Model of Drugs Involved in P-Glycoprotein Multidrug Resistance: Explanation of Structural Variety (Hypothesis)

Ilza K. Pajeva[†] and Michael Wiese^{*,‡}

Centre of Biomedical Engineering, Bulgarian Academy of Sciences, Academic George Bonchev Street Block 105, 1113 Sofia, Bulgaria, and Institute of Pharmacy, University of Bonn, An der Immenburg 4, 53121 Bonn, Germany

Received May 23, 2002

A general pharmacophore model of P-glycoprotein (P-gp) drugs is proposed that is based on a highly diverse data set and relates to the verapamil binding site of the protein. It is derived from structurally different drugs using the program GASP. The pharmacophore model consists of two hydrophobic points, three hydrogen bond (HB) acceptor points, and one HB donor point. Pharmacophore patterns of various drugs are obtained, and different binding modes are presumed for some of them. It is concluded that the binding affinity of the drugs depends on the number of the pharmacophore points simultaneously involved in the interaction with P-gp. On the basis of the obtained results, a hypothesis is proposed to explain the broad structural variety of the P-gp substrates and inhibitors: (i) the verapamil binding site of P-gp has several points that can participate in hydrophobic and HB interactions; (ii) different drugs can interact with different receptor points in different binding modes.

Introduction

The typical multidrug resistance (MDR) in tumor cells is associated with a decreased cellular drug accumulation achieved through ATP-dependent transport of the drugs out of cells by P-glycoprotein (P-gp).¹ P-gp is characterized by a broad structural and functional variety of its substrates and inhibitors (MDR modulators). The P-gp-related drugs belong to different chemical and biological classes, including anticancer agents, calcium channel blockers, neuroleptics, antiarrhythmics, antimalarial, antifungal, and many other drugs. Although most of these drugs share some common physicochemical and structural features, the structural parameters required for a molecule to be recognized and transported by P-gp are still unknown.

The pharmacophore models reported in the literature either relate to a strongly homologous series of compounds or utilize structurally diverse P-gp substrates and inhibitors tested for MDR reversal in vitro by different test systems in resistant tumor cells of different origin. The first definition of the MDR "pharmacophore" was based on structure–function relationships among reserpine and yohimbine analogues in the human leukemia cell line CEM/VLB100.^{2,3} Two planar aromatic domains and the disposition of basic nitrogen within an extended aliphatic chain were suggested as a conserved structural element of the MDR modulators. By analogy with binding of antipsychotic drugs to calmoduline, Hait and Aftab proposed a drug binding site on P-gp of phenothiazines and related drugs in human breast carcinoma MCF-7/DOX cells.⁴ In their model, the phenothiazine ring system was "sandwiched" by phenyl rings of the P-gp phenylalanine residues, whereas the drug's positively charged amino side chain

interacted with P-gp acidic residues. Suzuki et al. suggested π -hydrogen interactions for the aromatic rings in a quinoline series of modulators introducing additionally a prerequisite for a distance of at least 5 Å between the basic nitrogen and the center of the hydrophobic moiety formed by the aryl rings.⁵ Etievant et al. formulated requirements for P-gp recognition based on structure–activity relationships in the podophyllotoxin series and murine leukemic P388/ADR cells.⁶ Using the DISCO module, they showed that the position of the amido group relative to the trimethoxy aromatic ring (5 Å distance in the colchicine structure) associated with the charge density on the carbonyl appeared to be a predictive criterion for P-gp recognition. Seelig⁷ proposed a general pattern for P-gp substrate recognition formed by two or three electron donor groups with a fixed spatial separation of 2.5 ± 0.3 and 4.6 ± 0.6 Å, respectively. The pattern, however, is based on a comparison of P-gp substrates tested in different resistant cell lines without considering where and how the drugs bind to the protein.

In light of the current presentations on multiple binding sites of P-gp,⁸ the correct definition of the pharmacophore of P-gp-related drugs presumes availability of data on structurally diverse compounds that interact with the same binding site of P-gp. The earliest studies of structurally diverse substances recognized as P-gp substrates/modulators dealt mostly with simple IC₅₀ determinations and did not consider whether the compounds acted by the same mechanism and binding mode.⁹ Recently Litman et al. published the effect of 32 structurally diverse MDR substances on P-gp ATPase activity.¹⁰ In a series of papers, Doeppenschmitt et al.^{11–13} and Neuhoﬀ et al.¹⁴ reported on the affinity for the P-gp verapamil binding site of structurally different groups of compounds, including anticancer and MDR modulating drugs, their analogues, stereoisomers, and metabolites. The affinities of *R*- and *S*-enantiomers of

* To whom correspondence should be addressed. Phone: + 49 228 73 5212. Fax: +49 228 737929. E-mail: mwiese@uni-bonn.de.

[†] Bulgarian Academy of Sciences.

[‡] University of Bonn.

Table 1. Activity Data and pK_a Values of the Studied Compounds^a

compounds	affinity to the verapamil binding site ^{11,14}		ATP activity effect ¹⁰ two-affinity model K_1 , μM	pK_a values ^b	
	two-affinity model				
	K_{i1} , μM	f_1			
		one-affinity model IC_{50} , μM			
vinblastine	0.1	0.4	34.0	1.3	>N-(1): 7.59 ± 0.60 (e) 7.4^{17} >N-(2): 5.96 ± 0.70 (e) 5.4^{17}
rhodamine 123	0.1	0.7	0.5		=NH: 4.57 ± 0.40 -NH ₂ : 3.62 ± 0.40
verapamil (racemic)	0.3	0.4	1.48 ± 0.09 2.11 ± 0.47^c	2.5	>N-: 9.04 ± 0.50 ; (e) 8.92^{18} 8.68^{19}
<i>S</i> -verapamil			2.09 ± 0.35^c		
<i>R</i> -verapamil			2.37 ± 0.40^c	1.6	
norverapamil (racemic)			4.24 ± 0.32		>N-: 9.87 ± 0.19
haloperidol	0.2	0.3	5.3		>N-: 8.25 ± 0.40
ketoconazole	1.2	0.5	13.0		>N-(1): 5.41 ± 0.60
omeprazole			89.0 ± 13.8		>N-: 9.08 ± 0.30
<i>S</i> -omeprazole			91.2 ± 7.2		
<i>R</i> -omeprazole			97.2 ± 1.0		
quinidine	2.6	0.2	340.0	5.0	>N-: 9.13 ± 0.46 (e) 8.8^{17}
quinine	12.0	0.2	430.0		>N-: 9.13 ± 0.46 (e) 8.5^{17}
pafenolol	5.5	0.2			>N-(1): 9.18 ± 0.38
propranolol	48.0	0.5	573.0 ± 237		>N-: 9.15 ± 0.38
<i>S</i> -propranolol			574.0 ± 215	170.0	
<i>R</i> -propranolol			583.0 ± 151		
metoprolol	200	0.2	1300.0		>N-: 9.18 ± 0.38
reserpine				0.1	>N-: 7.25 ± 0.70
tamoxifen				0.1	>N-: 8.69 ± 0.28
amiodarone				3.2	>N-: 9.37 ± 0.25 (e) 8.7^{18}
propafenone				4.2	>N-: 9.31 ± 0.29
trifluoperazine				6.5	>N-(1): 4.04 ± 0.70 (sv) 7.61 ± 0.70 >N-(2): 7.81 ± 0.30 (e) 8.1^{18}
chlorpromazine	0.6	0.8		12.2	>N-: 9.41 ± 0.28 ; (e) 9.30^{18} 9.22^{19}
triflupromazine				15.7	>N-: 9.40 ± 0.28 ; (e) 9.20^{18} 9.07^{19}

^a K_{i1} , affinity constant for the high-affinity binding site of the human P-gp; f_1 , fraction of the high-affinity binding site; IC_{50} , drug concentration at 50% inhibition in one-affinity model; K_1 , drug concentration that gives half of the maximal ATPase activity calculated for the high-affinity binding site of the animal P-gp (see Figure 1 for the symbols of the atoms for which pK_a values are reported). ^b Calculated with ACD/pKa as apparent values; (sv) single pK_a ; ²⁰ (e) experimental pK_a . ^{17–19} ^c IC_{50} values obtained from different passages of cells.

some of these drugs were measured separately. These data appear as especially appropriate for the purpose of the pharmacophore definition of P-gp substrates and inhibitors because they involve structurally diverse compounds and stereoisomers whose affinity toward the same (verapamil) binding site of P-gp is quantitatively estimated.

In this work a general pharmacophore model is proposed for P-gp recognition by structurally diverse MDR substrates and modulators that bind to the verapamil binding site of the protein. The model was derived by means of a genetic algorithm similarity program GASP.¹⁵ Several pharmacophore points were identified: two hydrophobic, three hydrogen bond (HB) acceptor, and one HB donor points. Pharmacophore patterns of various drugs were derived, and different binding modes were suggested for some of them. It was concluded that the binding affinity of the drugs depended on the number of the pharmacophore points simultaneously involved in interaction with P-gp. The broad structural variety of the P-gp substrates and inhibitors that bind to the verapamil binding site of P-gp can be explained by the fact that the receptor has several points able to participate in hydrophobic and HB interactions; different drugs can occupy different receptor points in different binding modes.

Data and Methods

Activity and Physicochemical Data. The data from competition experiments with a radiolabeled [³H]-verapamil at the verapamil binding site of human carcinoma Caco-2 P-gp were taken from the publications of Doeppenschmitt et al.¹¹ and Neuhoff et al.¹⁴ In Table 1, the K_{i1} values characterizing the affinity of the ligands for the high-affinity site obtained by the two-affinity model and the IC_{50} values obtained by the one-affinity model are shown. Fraction f_1 of the high-affinity binding site is also included to give a presentation on the stoichiometry of the two-affinity model. The two-affinity model was statistically proven to be superior over the one-affinity model, though a significant correlation between K_{i1} and IC_{50} was observed.¹¹ In the table, drug concentrations K_1 are also shown that give half of the maximal increase in ATPase activity resulting from binding to the high-affinity (activating) binding site of CR1R12 Chinese hamster ovary P-gp.¹⁰ Additionally to the compounds from the verapamil binding set, several more drugs with ATPase effect were studied (Table 1, bottom). Although no data on the affinity to the verapamil binding site and ATPase activity effect were available for calcein-am (4'-bis(*N,N*-bis(carboxymethyl)aminomethyl) acetoxymethyl ester), this compound was also investigated as a widely used fluorescent

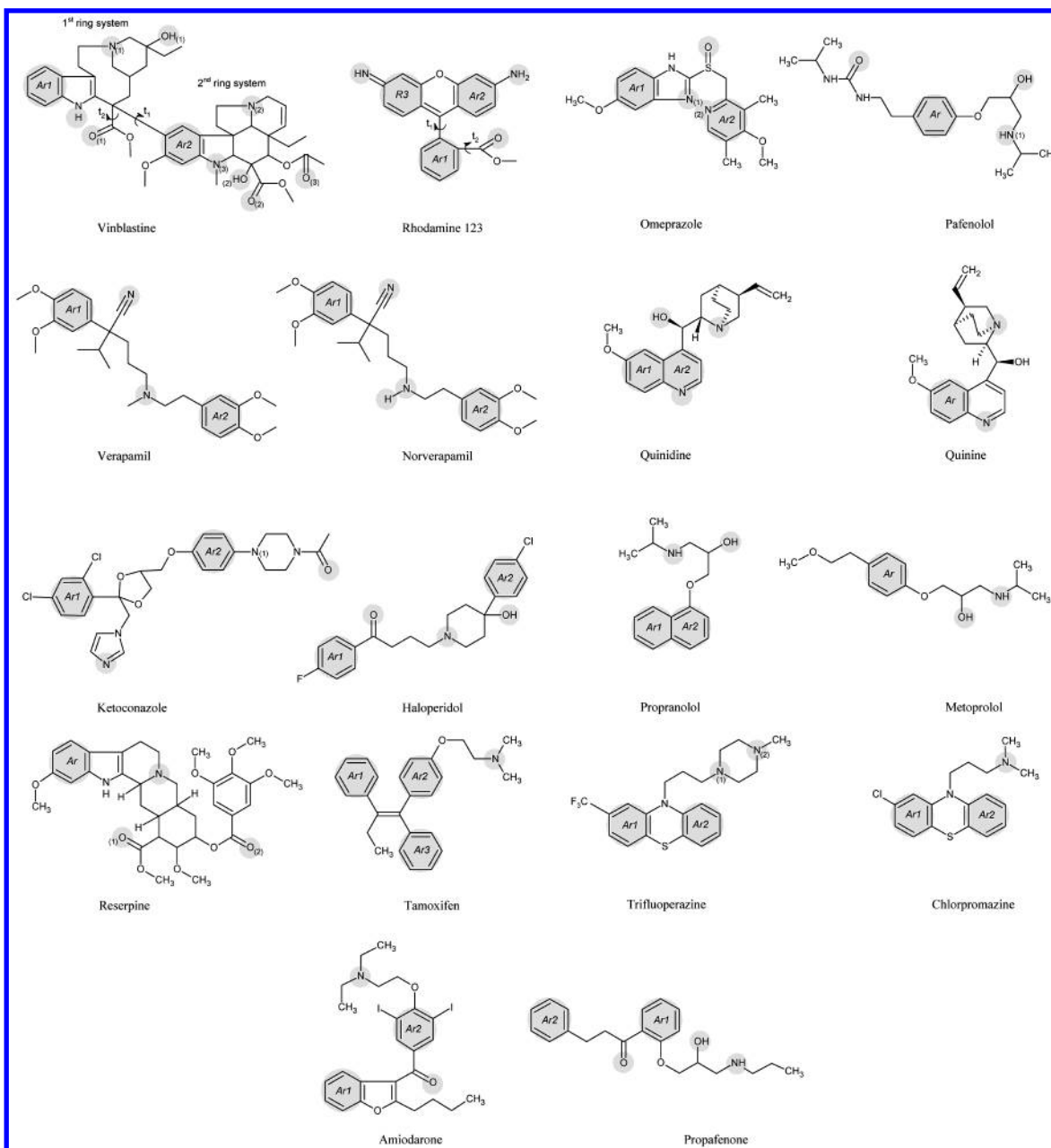


Figure 1. Structures of the studied drugs. Atoms and functional groups identified as pharmacophore points are shown in shaded circles (see Tables 2 and 4–7). t_1 and t_2 mark the rotatable bonds of vinblastine and rhodamine 123 used in the systematic search (see Experimental Section).

probe to rank the interaction between P-gp and various MDR drugs.¹⁶ The pK_a values given in Table 1 are either experimentally determined^{17–19} or calculated with the program ACD/pKa (see Methods). Each calculation is provided with its $\pm 95\%$ confidence limits.

The structures of the studied compounds are shown in Figure 1. From all the drugs listed in Table 1, only the structure of trifluopromazine is not shown as being very similar to that of chlorpromazine ($-\text{CF}_3$ instead of $-\text{Cl}$).

Methods. GASP¹⁵ and SYBYL molecular modeling software²⁰ were used. GASP requires no prior knowledge regarding either the receptor or the pharmacophore pattern. It performs automatic pharmacophore elucidation with full conformational flexibility of the ligands. Considering that the 3D structure of the P-gp MDR receptor is unknown and that most of the MDR

modulators are small and conformationally flexible molecules, GASP appears as a suitable tool to study the P-gp-related drugs in order to elucidate their common pharmacophore pattern. The program employs a genetic algorithm for determining the correspondence between functional groups in the superimposed ligands and the alignment of these groups in a common geometry for receptor binding. All aromatic rings and HB sites are automatically recognized as potential pharmacophore elements. A population of chromosomes is randomly constructed with each chromosome representing a possible alignment. Torsion angles for the rotatable bonds are adjusted when searching for molecule alignment. The fitness score of a given alignment is a weighted sum of three terms: the number and similarity of the overlaid elements, the common volume of the molecules, and the internal van der Waals (vdW) energy of each

molecule. The calculation terminates when the fitness of the population does not further improve by a specified value or when the preset number of genetic operations is completed.

Compounds were studied in a pairwise comparison, and the 10 best alignments were analyzed. Because the GASP algorithm uses random numbers for initialization, all pairs were run more than once to estimate the reproducibility of the obtained overlays. The settings of the GASP parameters are described in the Experimental Section.

The pK_a values were calculated with the program ACD/pKa, version 5.0, using the ACD/I-Lab service.²¹ The so-called "apparent constants" were calculated where the algorithm mimics the experimental order of protonation and determines the pK_a values, which can be really experimentally measured in water solution. For purposes of comparison, "single" pK_a values were also computed that relate to single dissociation centers when the rest of the molecule was considered neutral. In most cases, almost equal values were obtained by both approaches. Slight differences were observed for pK_a values far above or far below 7.4. The single pK_a is separately reported only for trifluoperazine in which the nitrogen atom $>N-(1)$ (Figure 1) possesses a single pK_a significantly different from the apparent one (Table 1).

Results

There are two key factors in developing a pharmacophore model by GASP: (i) selection of the template ligand and (ii) determination of the functional groups essential for binding. Because the program allows molecules to flex during the alignment onto a fixed template, the right choice of the template conformation is crucial. Equally important is the use of the proper ionization rule for the drug at the binding conditions of interest. Most of the studied drugs contain tertiary nitrogens that can be either neutral (in membrane environment) or protonated to a different extent at physiological pH. To decide on the right ionization state of the drugs, the pK_a values of the nitrogen atoms were taken into account (Table 1). In the study, both the neutral and the monoprotonated forms of the compounds were investigated.

Selection of the Template Ligand. There were two potential template candidates in the data set: vinblastine and rhodamine 123. Vinblastine is an anticancer drug and a well-recognized P-gp substrate. It was also shown to be the more active inhibitor of binding of a photoactive analogue of verapamil to P-gp compared to an anthracycline doxorubicin.²² Rhodamine 123 is a specific substrate for P-gp too and is shown to be the preferred substrate for studying P-gp functionality in Caco-2 cells.²³ In the radioligand binding assay data, vinblastine and rhodamine 123 have the highest affinity for the high-affinity site (0.1 μ M) in the two-affinity model; however, the fraction f_1 of vinblastine is about twice lower than that of rhodamine 123. Thus, in the one-affinity model, vinblastine is less active than rhodamine 123 (34 versus 0.5 μ M) (Table 1). In comparison to all other compounds reported to bind to the verapamil binding site of P-gp, vinblastine and rhodamine 123 have the most rigid structures. Therefore, in the study, both vinblastine and rhodamine 123 were experimented as template molecules.

Identification of the Essential Functional Groups. Vinblastine and rhodamine 123 (Figure 1) have several functional groups that can be involved in interactions with P-gp. Since no information about the right conformations of these ligands at the P-gp binding site was available, the energy minimum conformers of the drugs (see the Experimental Section) were studied in a pairwise manner using rhodamine 123 and vinblastine as fitted and template molecules conversely. Because it is not clear whether the drugs bind to P-gp in a neutral or ionized form, both were considered. Two monoprotonated forms of vinblastine were investigated. According to the pK_a values, $>N-(1)$ is considered as an initially protonated nitrogen at physiological pH; the experimental pK_a is 7.4, and the calculated value, apparent and single, is 7.59 (Table 1). To avoid a possible mistake with the pK_a assignments, $>N-(2)$ was also considered as a positively charged nitrogen (experimental pK_a of 5.4; calculated apparent and single value of 5.96). The tertiary nitrogen of rhodamine 123 is not charged at pH 7.4 ($pK_a = 3.62$), and correspondingly, no ionized form of it was considered.

Rhodamine 123. A total of 40 GASP runs (400 alignments) were performed with rhodamine 123 aligned on the neutral and monoprotonated forms of vinblastine. The two global minimum conformers of rhodamine 123 (R123-1 and R123-2) were overlaid on each of the energy minimum conformers of vinblastine Vnbl-1, Vnbl-2, Vnbl-3, and Vnbl-4 (see the Experimental Section for a description of the conformers). The results are summarized in Table 2. The highest fitness scores were obtained on Vnbl-1 and Vnbl-2 (from 2962 to 3240). Vnbl-3 and Vnbl-4 produced alignments that had scores at the rate of 2500. As seen from the table, the most frequently observed patterns of rhodamine 123 (shown in bold) on Vnbl-1 involved all the functional groups of the target while those obtained with the other vinblastine conformers involved fewer atoms and functional groups, mainly from the second ring system of vinblastine (Figure 1). Vnbl-1 was the template that steadily involved the two aromatic rings and had a common volume held well by both molecules. Vnbl-2 gave overlays with the two aromatic rings more often than Vnbl-3 and Vnbl-4, in agreement with its conformational similarity to Vnbl-1 (see the Experimental Section). In Figure 2A, the five-point overlay of rhodamine 123 on Vnbl-1 is shown. As seen from the figure, there is an excellent correspondence between the spatial arrangement of the identified pharmacophore elements and the directionality of their interactions with the putative receptor points. The identified pharmacophore points were coded as follows: two hydrophobic centers H_1 and H_2 , two HB acceptor points A_1 and A_2 , and one HB donor point D_A . They corresponded respectively to Ar1, Ar2, =O₍₁₎, N₍₃₎, and OH₍₁₎ of vinblastine and Ar1, R3 or Ar2, =O, =NH, and -NH₂ or =NH of rhodamine 123 (Figure 1, Table 2). The most steadily involved functional groups of vinblastine were the aromatic rings, =O₍₁₎ and -OH₍₁₎. Besides $>N-(3)$, =O₍₂₎ and -OH₍₂₎ were also identified as HBacceptors producing closely located receptor points. This suggests that A_2 could be a flexible pharmacophore point: atoms in conformationally flexible functional groups located close to $>N-(3)$ can be involved as A_2 , e.g., =O₍₂₎, =O₍₃₎, and -OH₍₂₎. Involve-

Table 2. Pharmacophore Patterns of the Energy Minimum Conformers of Rhodamine 123 (R123) Identified in Overlays on the Energy Minimum Conformers of the Neutral and Monoprotonated Forms of Vinblastine (Vnbl)^a

pharmacophore points template = Vnbl targets = R123-1 and -2								
	hydrophobic		HB acceptors				HB donors	
Vnbl-1	Ar1	Ar2	=O ₍₁₎	>N ₋₍₃₎	-OH ₍₂₎	=O ₍₂₎	-OH ₍₁₎	>NH
	Ar1	R3	= O	= NH			= NH₂	
	Ar1	Ar2	=O		=O		=NH	-NH ₂
Vnbl-2	Ar1	Ar2	=O ₍₁₎	>N ₋₍₃₎	-OH ₍₂₎	=O ₍₂₎	-OH ₍₁₎	>NH
		Ar2			= O			= NH₂
	Ar1	R3	=O	=NH			-NH ₂	
Vnbl-3	Ar1	Ar2	=O ₍₁₎	>N ₋₍₃₎	-OH ₍₂₎	=O ₍₂₎	-OH ₍₁₎	>NH
		R3			= O	= NH		
		Ar2			=O ^b			
Vnbl-4	Ar1	Ar2	=O ₍₁₎	>N ₋₍₃₎	-OH ₍₂₎	=O ₍₂₎	-OH ₍₁₎	>NH
					= O^b	= NH		= NH₂
	Ar1	Ar2	=O		=O ^b			
Vnbl-1N ₁ ⁺	Ar1	Ar2	=O ₍₁₎	>N ₋₍₃₎	-OH ₍₂₎	=O ₍₂₎	-OH ₍₁₎	>NH
	Ar1	R3	= O	= NH			= NH₂	
	Ar1	Ar2	=O				=NH	
Vnbl-1N ₂ ⁺	Ar1	Ar2	=O ₍₁₎	>N ₋₍₃₎	-OH ₍₂₎	=O ₍₂₎	-OH ₍₁₎	>NH
	Ar1	R3	= O	= NH			= NH₂	
	Ar1	Ar2	=O					

^a The most frequently observed pharmacophore patterns are shown in bold (see Experimental Section for a description of the template and target conformations and Figure 1 for symbols of atoms and functional groups that appear as pharmacophore points). ^b Two electron pairs of the oxygen atom involved in HB acceptor interactions.

Table 3. Energies and Geometrical Characteristics of Rhodamine 123^a

conformation	energy, kcal/mol	torsions, deg ^b		distances between the pharmacophore points, Å									
		t ₁	t ₂										
				H ₁ -A ₁	H ₁ -A ₂	H ₁ -D _A	H ₂ -A ₁	H ₂ -A ₂	H ₂ -D _A	H ₁ -H ₂	A ₁ -A ₂	A ₁ -D _A	A ₂ -D _A
GASP-5	19.505	110.7	-127.8	3.665	7.406	8.406	5.198	2.689	7.623	4.958	7.218	8.628	9.559
GASP-5m	4.137	110.3	171.8	3.670	7.405	8.438	4.942	2.704	7.606	4.958	6.810	9.384	9.559
GASP-4	12.514	-73.5	-136.3	3.665	<i>c</i>	8.237	5.393	<i>c</i>	7.555	5.046	<i>c</i>	8.428	<i>c</i>
GASP-4m	3.941	-68.1	172.0	3.673	<i>c</i>	8.286	5.014	<i>c</i>	7.559	5.046	<i>c</i>	9.232	<i>c</i>
R123-1	3.931	-67.9	171.7	3.670	<i>c</i>	8.235	4.999	<i>c</i>	7.556	5.051	<i>c</i>	9.244	<i>c</i>
R123-2	3.931	67.5	-171.1	3.666	7.418	8.395	6.191	2.717	7.604	4.944	8.631	7.588	9.669

^a GASP-5 and GASP-4 are the conformations of the five- and four-point pharmacophore models obtained by GASP on vinblastine (see Table 2). GASP-5m and GASP-4m are the minimized conformations (Tripos force field, Powell method, Gastheiger-Hückel charges, 0.05 kcal mol⁻¹ Å⁻¹ convergence). R123-1 and R123-2 are the global minimum conformers. ^b Measured in the range of -180° to 180°. ^c No A₂ involved.

ment of >NH in HB donor interactions was observed in 3 out of 16 pharmacophore patterns and mostly in overlays that held a bad common volume between the drugs. Overlays of rhodamine 123 on the protonated >NH⁺₋₍₁₎ and >NH⁺₋₍₂₎ forms of vinblastine resulted in the same patterns as the neutral ones (Table 2). Neither of the ionized nitrogens was involved as a pharmacophore point in the resulting alignments.

To decide on the relevance of the resulting GASP conformations of rhodamine 123, the five- and four-point models were analyzed in more detail. In Table 3 the energies and geometrical characteristics (torsions and distances) of rhodamine 123 conformations obtained from the GASP five- and four-point models are shown

(alignments with high scores were selected and were respectively coded GASP-5 and GASP-4). The minimized forms are also given (GASP-5m and GASP-4m). The global minimum conformers of R123-1 and R123-2 are included for comparison. GASP-4m resembles more closely R123-1, while GASP-5m resembles R123-2 better. The distances between the main pharmacophore points in GASP-5 and GASP-5m and in GASP-4 and GASP-4m are very close. At the same time, the differences in the energies of the minimized conformations and those of the global conformers are 0.21 kcal/mol (GASP-5m) and 0.01 kcal/mol (GASP-4m), suggesting that these conformations have energetically reasonable geometries.

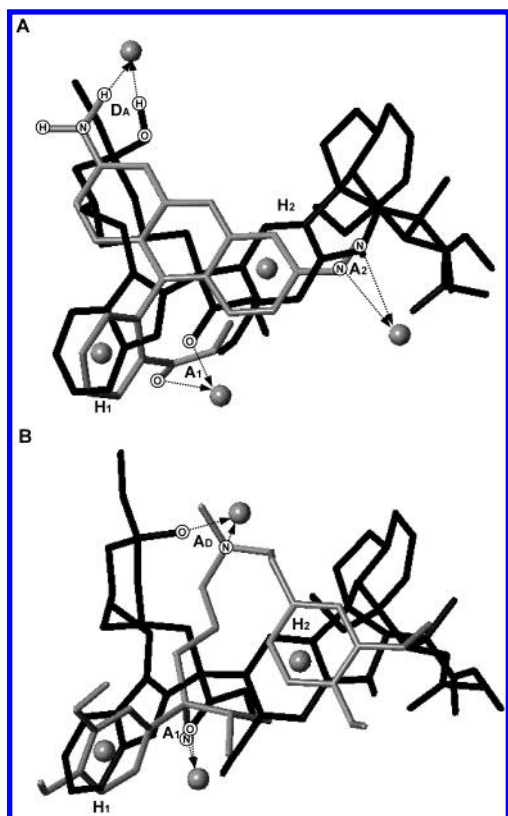


Figure 2. Overlay of (A) rhodamine 123 and (B) *R*-verapamil (in gray) on vinblastine (in black) obtained by GASP for the unprotonated drugs. H₁ and H₂ are hydrophobic points (shown as balls) located around the centers of the aromatic rings; A₁, A₂, and A_D are HB acceptor points; D_A is a HB donor point; the complementary HB donor and acceptor points of the receptor are represented also as balls at a distance of about 2.9 Å from the acceptor or donor atom of the drug in the direction of lone pair or hydrogen. The arrows show directions of the HB interactions. Only heteroatoms and hydrogens are shown that appear as HB acceptor and donor points (see also Figure 1 and Tables 2–4 for the atoms and functional groups involved).

From the above results, it can be concluded that the overlays on Vnbl-1 involve most functional groups of both rhodamine 123 and vinblastine and ensure the best common volume between the overlaid molecules. Up to five pharmacophore points might be involved in the interaction of the drugs at the verapamil binding site of the protein. The five- and four-point pharmacophore patterns of rhodamine 123 are based on conformations with energetically reasonable geometries and may reflect two different binding modes of rhodamine 123.

Vinblastine. To further decide on the most suitable template and the potential pharmacophore points, the overlays were also analyzed using rhodamine 123 as a template. Table 4 summarizes the pharmacophore patterns of vinblastine among 26 runs resulting in 260 alignments in the fitness score interval 2849–3255. As seen from the table, the most frequently observed patterns of Vnbl-1 on R123-1 and R123-2 reproduced those of rhodamine 123 on Vnbl-1 (Table 2). Vnbl-2 gave patterns similar to those of Vnbl-1, while Vnbl-3 and Vnbl-4 produced mostly patterns with one hydrophobic center involved. Analysis showed that the first ring system of vinblastine held no common volume with rhodamine 123 in these alignments. Although with much lower appearance, Vnbl-3 and Vnbl-4 also gave

patterns that involved Ar1, Ar2, and =O₍₁₎. In general, the pattern with Ar1, Ar2, and =O₍₁₎ was reproduced by all vinblastine conformers (Table 4). In a number of patterns, additionally to >N₍₃₎, the –OH₍₂₎, =O₍₂₎, and =O₍₃₎ appeared as the HB acceptor point A₂. Thus, the possible participation of HB acceptor groups other than >N₍₃₎ as the pharmacophore point A₂ was confirmed again. The –OH₍₁₎ group of vinblastine appeared again as an HB donor overlaid on either the =NH or –NH₂ group of rhodamine 123. Overlays of the ionized forms of vinblastine did not involve any of the protonated nitrogens of vinblastine. Patterns as observed for the neutral forms were obtained.

Thus, in the overlays of vinblastine (neutral and protonated) on the rhodamine 123 conformers, the same patterns were reproduced as identified in the overlays of rhodamine 123 on Vnbl-1 (Table 2).

Verapamil. Considering that affinity to the verapamil binding site of P-gp was measured and that *K*_{i1} of verapamil is among the lowest (Table 1), a number of alignments were also produced with *S*- and *R*-verapamil on either vinblastine or rhodamine 123 templates. All vinblastine and rhodamine 123 conformers were experimented as templates. Diverse pharmacophore patterns were observed in agreement with the high conformational flexibility of verapamil. Selection of the most appropriate patterns was done on the basis of the fitness score and frequency of occurrence of the same pattern in different runs. The number of the identified pharmacophore points and the common volume held by the overlaid molecules were taken into account. The results of 36 runs on the vinblastine template are summarized in Table 5A. Only the overlays on the lowest energy conformers Vnbl-1 and Vnbl-2 are shown because they produced pharmacophore patterns with the highest scores and frequency of appearance and involved the most functional groups of verapamil simultaneously. The fitness scores varied from 3491 to 4193. As seen from the table, the neutral form of verapamil shows several pharmacophore patterns that involve its functional groups in different combinations: the hydrophobic centers Ar1 and Ar2 and the HB acceptors of the cyano ≡N and the tertiary nitrogen >N– atoms (Figure 1). Again, the same points as observed in overlays between rhodamine 123 and vinblastine were recorded, namely, Ar1, Ar2, =O₍₁₎ corresponding to the hydrophobic centers H₁ and H₂, and the HB acceptor point A₁. However, a new HB acceptor point overlaid on the oxygen atom in –OH₍₁₎ of vinblastine appeared. Figure 2B illustrates one of the observed patterns of *R*-verapamil on vinblastine. H₁, H₂, and A₁ are the same as in the overlay of rhodamine 123 (Figure 2A) involving Ar1, Ar2, and ≡N of verapamil. The tertiary >N– of verapamil is overlaid on OH₍₁₎ of vinblastine with the oxygen atom acting as an acceptor. The new point is labeled by A_D reflecting the dual role of the –OH₍₁₎ group of vinblastine that can act as both an acceptor and a donor simultaneously. Patterns were also observed that involved the A₂ point: >N– and ≡N of verapamil on either >N₍₃₎ or =O₍₂₎ of vinblastine. In the overlays on Vnbl-2, >N₍₁₎ of vinblastine was also identified as an HB acceptor point similarly to the –OH₍₁₎. The *R*- and *S*-enantiomers resulted in the same patterns (Table 5A). Figure 3 illustrates two pharma-

Table 4. Pharmacophore Patterns of the Energy Minimum Conformers of Vinblastine (Vnbl) Identified in Overlays on the Energy Minimum Conformers of Rhodamine 123 (R123)^a

	pharmacophore points template = R123-1 and -2 target = Vnbl						
	H ₁	H ₂	H ₂	A ₁	A ₂	D _A	D _A
R123-1	Ar1	Ar2	R3	=O	=NH	=NH	-NH ₂
Vnbl-1	Ar1	Ar2	Ar2	=O₍₁₎	>N₍₋₃₎	=NH	-OH₍₁₎
Vnbl-2	Ar1	Ar2	Ar2	=O₍₁₎	>N₍₋₃₎	-OH₍₁₎	
Vnbl-3	Ar1	Ar2		=O ₍₁₎	=O ₍₂₎ or =O ₍₃₎		>NH
Vnbl-4	Ar1	Ar2		=O ₍₁₎		-OH ₍₁₎	>NH
Vnbl-1N ₁ ⁺ and Vnbl-1N ₂ ⁺	Ar1	Ar2	Ar2	=O ₍₁₎	>N ₍₋₃₎	-OH ₍₁₎	-OH ₍₁₎
R123-2	Ar1	Ar2	R3	=O	=NH	=NH	-NH ₂
Vnbl-1	Ar1		Ar2	=O₍₁₎	-OH₍₂₎		-OH₍₁₎
Vnbl-2	Ar1		Ar2	=O ₍₂₎			>NH
Vnbl-3		Ar2	Ar2	=O₍₁₎	-OH₍₂₎		-OH₍₁₎
Vnbl-4	Ar1	Ar2	Ar2	=O ₍₂₎			>NH
Vnbl-1N ₁ ⁺ and Vnbl-1N ₂ ⁺	[Ar1]		Ar2	=O ₍₂₎ or =O ₍₃₎	>N ₍₋₃₎		>NH
	Ar1		Ar2	=O ₍₁₎			>NH
		Ar2		=O ₍₂₎			>NH
				=O ₍₁₎	>N ₍₃₎		-OH ₍₁₎
				=O₍₁₎	-OH₍₂₎		-OH₍₁₎
				=O ₍₂₎			>NH

^a H₁, H₂, hydrophobic centers; A₁, A₂, HB acceptors; D_A, HB donor. The most frequently observed pharmacophore patterns are shown in Bold (see Experimental Section for a description of the template and target conformations and Figure 1 for symbols of atoms and functional groups that appear as pharmacophore points).

cophore patterns of verapamil corresponding to two possible binding modes in which either ≡N or >N- can be A₁ or A_D acceptors or conversely. No HB donor was recorded in the overlays of the neutral forms.

The overlays of the protonated forms kept the combination of H₁, H₂, and A₁; however, instead of the acceptor point A_D, an HB donor point appeared involving the protonated nitrogen of verapamil overlaid on hydrogen atoms of either -OH₍₁₎ or >NH₍₋₁₎⁺ (Table 5A). In contrast to the overlays with rhodamine 123, in the case of verapamil, the >NH₍₋₁₎⁺ group of vinblastine also appeared as a HB donor. In the overlays on the monoprotonated >NH₍₋₂₎⁺ forms of vinblastine, no involvement of the positively charged nitrogen was registered and the produced patterns resembled fully the patterns of the neutral ones.

In Table 5B the pharmacophore patterns of verapamil obtained on the rhodamine 123 template are shown. The same points as observed in the above overlays were recorded: H₁, H₂, and A₁, corresponding to Ar1, R3 or Ar2, and =O of rhodamine 123. The HB acceptor point A_D was also identified for the acceptor functions of the >N- atom of verapamil and the =NH group of rhodamine 123, suggesting a dual role of the =NH group. It should be noted, however, that the direction of the A_D interaction was opposite to that observed with the -OH₍₁₎ group of vinblastine in correspondence with the lone pair direction in the planar geometry of the nitrogen atom in the =NH group. In the overlays of the protonated forms, the D_A point involved the hydrogen atoms of the protonated nitrogen of verapamil and the -NH₂ group of rhodamine 123.

The results with verapamil point to involvement of another HB acceptor pharmacophore point A_D in the pharmacophore pattern of drugs at the verapamil binding site of P-gp. Additionally, the hydrogen atoms of the

protonated nitrogens of verapamil and vinblastine (>NH₍₋₁₎⁺) were identified as D_A HB donors. Different pharmacophore patterns that involved all functional groups of verapamil were recorded corresponding to possibly different binding modes of the drug. The similar patterns of the *R*- and *S*-forms obtained suggest a similar way of binding of the enantiomers in agreement with their equal affinity to P-gp.

Conclusions about the Template and the Potential Pharmacophore Points. The analysis of the above overlays points to vinblastine as an appropriate template molecule. The same pharmacophore patterns were identified in both target and template overlays with rhodamine 123, suggesting that vinblastine was able to produce robust pharmacophore patterns. At the same time, rhodamine 123 showed two equally reasonable pharmacophore patterns. The vinblastine molecule is much larger than that of rhodamine 123 and possesses more functional groups. In contrast to rhodamine 123, it contains tertiary nitrogens that can be protonated at physiological pH, which appears to be a common feature for many P-gp-related drugs and gives, in this way, a possibility for investigation of the drug-protonated forms too. Finally, *K*_{H1} of vinblastine is similar to that of rhodamine 123 but at about double the lower binding site fraction (Table 1). All these facts point to vinblastine as the most relevant template among the available drugs for identification of the pharmacophore patterns of P-gp drugs. Thus, in further alignments, the global minimum conformers Vnbl-1 of the neutral and >N₍₋₁₎ monoprotonated forms of vinblastine were used as templates.

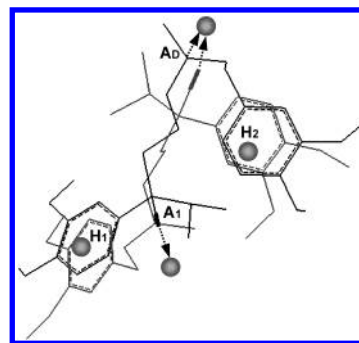
The main points identified in the overlays between the most active drugs can be summarized as follows: two hydrophobic centers H₁ and H₂, three HB acceptor points A₁, A₂, A_D, and one HB donor point D_A. H₁, H₂,

Table 5. Pharmacophore Patterns of Verapamil Enantiomers Identified in Overlays on the Energy Minimum Conformers of (A) Vinblastine (Vnbl) and (B) Rhodamine 123 (R123)^a

(A) Pharmacophore Patterns Template = Vinblastine Target = Verapamil						
	H ₁	H ₂	A ₁	A ₂	A _D	A _D
Vnbl-1	Ar1	Ar2	=O ₍₁₎	>N ₍₋₃₎	=O ₍₂₎	-OH ₍₁₎
<i>S</i> -verapamil	Ar1	Ar2	≡N			>N-
	Ar2	Ar1	>N-		≡N	
	Ar2	Ar1				≡N
	Ar1		≡N	>N-		
<i>R</i> -verapamil	Ar1	Ar2	≡N			>N-
	Ar2	Ar1	>N-			≡N
	Ar2	Ar1	≡N			
	Ar2			≡N		>N-
	H ₁	H ₂	A ₁	A ₂	A _D	A _D
Vnbl-2	Ar1	Ar2	=O ₍₁₎		-OH ₍₁₎	>N ₍₋₁₎
<i>S</i> -verapamil	Ar1	Ar2	≡N		>N-	
	Ar2	Ar1	≡N		>N-	
<i>R</i> -verapamil	Ar2	Ar1	≡N			
	Ar1		≡N	>N-		
	H ₁	H ₂	A ₁	A _D	D _A	D _A
Vnbl-1N ₁ ⁺	Ar1	Ar2	=O ₍₁₎		-OH ₍₁₎	>NH ₍₁₎ ⁺
<i>S</i> -verapamil (protonated)	Ar1	Ar2	≡N			>NH ⁺
	Ar1	Ar2	≡N			
<i>R</i> -verapamil (protonated)	Ar1	Ar2	≡N			>NH ⁺
	Ar2	Ar1	≡N			>NH ⁺
Vnbl-1N ₂ ⁺	Ar1	Ar2	=O ₍₁₎		-OH ₍₁₎	>NH ₍₂₎ ⁺
	Ar1	Ar2	≡N		>NH ⁺	
<i>S</i> -verapamil (protonated)	Ar2	Ar1	≡N			
	Ar2	Ar1	≡N		>NH ⁺	
(B) Pharmacophore Patterns Template = Rhodamine 123 Target = Verapamil						
	H ₁	H ₂	H ₂	A ₁	A _D	D _A
R123-1	Ar1	Ar2	R3	=O	=NH	-NH ₂
<i>S</i> -verapamil	Ar1	Ar2		≡N	>N-	
			Ar2	≡N		
		Ar1		≡N	>N-	
<i>R</i> -verapamil	Ar1	Ar2		≡N	>N-	
	Ar1		Ar2	≡N		
<i>S</i> -verapamil and <i>R</i> -verapamil (protonated)	Ar1	Ar2		≡N		>NH ⁺
	Ar1		Ar2	≡N		
	Ar1	Ar2		≡N		
R123-2	Ar1	Ar2	R3	=O	=NH	-NH ₂
<i>S</i> -verapamil	Ar1	Ar2		≡N	>N-	
	Ar1		Ar2	≡N		
<i>R</i> -verapamil	Ar1		Ar2	≡N		
<i>S</i> -verapamil (protonated)			Ar2	≡N		>NH ⁺
	Ar1		Ar2	≡N		
<i>R</i> -verapamil (protonated)	Ar1	Ar2		≡N		>NH ⁺
	Ar1			≡N		>NH ⁺

^a See Experimental Section for a description of the template and target conformations and Figure 1 for symbols of atoms and functional groups that appear as pharmacophore points.

and A₁ were associated with the same atoms and groups in vinblastine and rhodamine 123. H₂ was related to either Ar2 or R3 of rhodamine 123. The A₂ point was mostly related to >N₍₃₎, but also =O₍₂₎, =O₍₃₎, and -OH₍₁₎ of vinblastine were involved. The -OH₍₁₎ group of vinblastine and =NH group of rhodamine 123 were identified as either A_D or D_A points, presuming their dual role in binding. As will be further shown, although no A_D was identified in the overlays between vinblastine

**Figure 3.** Main pharmacophore patterns of *R*-verapamil as obtained by GASP alignments on vinblastine. H₁ and H₂ are the hydrophobic points located around the centers of the aromatic rings that correspond to either Ar1 or Ar2. A₁ and A_D are the acceptor points that correspond to either tertiary >N- or cyano ≡N of verapamil. Pattern 1 is H₁(Ar1), H₂(Ar2), A₁(≡N), A_D(>N-); pattern 2 is H₁(Ar2), H₂(Ar1), A₁(>N-), A_D(≡N) (see Figure 1 and Table 4 for pharmacophore points and patterns observed).

and rhodamine 123, this does not exclude the possibility of simultaneous participation of A_D and D_A points in the pharmacophore pattern of the P-gp-related drugs. Although rare, in vinblastine, >N₍₋₁₎ appeared as an A_D point instead of the oxygen atom in -OH₍₁₎. The protonated nitrogen of vinblastine was identified as a D_A point with verapamil, demonstrating that depending on the protonation state, the same atom can function as an acceptor or donor keeping a similar topology of the neutral and protonated pharmacophore patterns. The possibility of different but closely located atoms, which belong to conformationally flexible groups, acting as A₂, A_D, and D_A points suggested that these might be flexible pharmacophore points.

P-gp Drugs (Radioligand Binding Assay Data).

The results of overlays of drugs that interact with the verapamil binding site of P-gp are summarized in Table 6. The main pharmacophore patterns of rhodamine 123 and verapamil are also included for a better overview of the patterns of the studied modulators. Part A of the table represents the results with the neutral drug forms. The fitness scores varied from drug to drug, being in the intervals 2832–3045 for haloperidol, 3562–3979 for ketoconazole, 2882–3115 for quinidine and quinine, and 2743–2924 for chlorpromazine. As seen from the table, the pharmacophore points identified with rhodamine 123 and verapamil were also obtained with the other drugs in different combinations. The mostly observed points were again H₁, H₂, and A₁. A₂ appeared mainly overlaid on -OH₍₂₎ of vinblastine (haloperidol, ketoconazole, quinidine, pafenolol, metropolol) but also on >N₍₋₃₎ (quinidine) and =O₍₂₎ (ketoconazole). In the neutral forms, the donor point D_A appeared when a relevant group was present; in most cases it involved a group that could act as an acceptor and donor simultaneously, e.g., -OH, -NH- (quinidine, pafenolol, propranolol). Similarly to verapamil, the same patterns for the enantiomers of omeprazole, propranolol, and metoprolol were obtained in agreement with the experimental data (Table 1).

Table 6B represents the pharmacophore patterns of the protonated drugs overlaid on the >N₍₋₁₎ charged form of vinblastine. Runs were also performed with the >N₍₋₂₎ charged form, but the patterns of the neutral

Table 6. Pharmacophore Patterns of MDR Drugs That Bind to the Verapamil Binding Site of P-gp Identified in Overlays on Neutral (A) and Protonated (B) Forms of Vinblastine^a

(A) On Neutral Form of Vinblastine								
compound	<i>n</i>	pharmacophore points						
		H ₁	H ₂	A ₁	A ₂ ^b	A _D	D _A	D _A
vinblastine	6	Ar1	Ar2	=O ₍₁₎	1, 2, 3	-OH ₍₁₎	>N ₋₍₁₎	-OH ₍₁₎
rhodamine 123	5	Ar1	R3	=O	=NH/1			-NH ₂
verapamil	4	Ar1	Ar2	=O				=NH
	4	Ar1	Ar2	≡N		>N-		
	4	Ar2	Ar1	>N-		≡N		
	4	Ar2	Ar1	>N-	≡N/1			
	4	Ar2	Ar1	≡N	>N-/3			
norverapamil	3	Ar1		≡N			>N-	
	4	Ar1		≡N		>NH		>NH
	3	Ar1	Ar2	≡N				
	3	Ar2	Ar1			≡N		
	3		Ar1	≡N				>NH
haloperidol	4	Ar2	Ar1	>N-		=O		
	3	Ar2	Ar1	=O				
	3	Ar1		=O		>N-		
	3	Ar2		-OH	=O/2			
	4	Ar1	Ar2		=O/2	=N-		
ketoconazole	4	Ar1	Ar2		=O/3	=N-		
	3	Ar1	Ar2	=N-				
	3	Ar1	Ar2			=N-		
	3	Ar1	Ar2	=O		=N ₋₍₂₎		
	4	Ar1	Ar2	=O			=N ₋₍₁₎	
omeprazole	3	Ar1	Ar2			=O		
	4	Ar1	Ar2			>N-		
	3		Ar1			>N-		
	3		Ar		=N-/2	>N-		
	3		Ar			-OH		-OH
quinidine	3		Ar	=O	>NH _{(1)/2}			-OH
	3		Ar2			-OH		-OH
	3		Ar2			-NH		-OH
	3		Ar1			-OH		-OH
	3		Ar					-OH
quinine	3		Ar					-OH
	3		Ar					-OH
	3		Ar					-OH
	3		Ar					-OH
	3		Ar					-OH
pafenolol	3		Ar					-OH
	3		Ar					-OH
	3		Ar					-OH
	3		Ar					-OH
	3		Ar					-OH
propranolol	3		Ar					-OH
	3		Ar					-OH
	3		Ar					-OH
	3		Ar					-OH
	3		Ar					-OH
metoprolol	3		Ar					-OH
	3		Ar					-OH
	3		Ar					-OH
	3		Ar					-OH
	3		Ar					-OH

(B) On Protonated Form of Vinblastine

compound	<i>n</i>	pharmacophore points						
		H ₁	H ₂	A ₁	A _D	D _A	D _A	D _A
vinblastine	5	Ar1	Ar2	=O ₍₁₎	-OH ₍₁₎	>NH ₍₁₎ ⁺		-OH ₍₁₎
verapamil	4	Ar1	Ar2	≡N		>NH ⁺		
	4	Ar1	Ar2	≡N				>NH ⁺
	4	Ar2	Ar1	≡N		>NH ⁺		
	4	Ar2	Ar1	≡N				>NH ⁺
	4	Ar1	Ar2	=O		>NH ⁺		
haloperidol	4	Ar1	Ar2	=O		>NH ⁺		
quinidine	4		Ar2		-OH	>NH ⁺		-OH
	3		Ar1	-OH		>NH ⁺		
	3		Ar1	-OH		>NH ⁺		
	3		Ar	-OH		>NH ⁺		
	3		Ar	-OH		>NH ⁺		
quinine	3		Ar	-OH		>NH ⁺		
	3		Ar	-OH		>NH ⁺		
	3		Ar	-OH		>NH ⁺		
	3		Ar	-OH		>NH ⁺		
	3		Ar	-OH		>NH ⁺		
pafenolol	3		Ar	-OH		>NH ⁺		
	3		Ar	-OH		>NH ⁺		
	3		Ar	-OH		>NH ⁺		
	3		Ar	-OH		>NH ⁺		
	3		Ar	-OH		>NH ⁺		
propranolol	3		Ar	-OH		>NH ⁺		
	3		Ar	-OH		>NH ⁺		
	3		Ar	-OH		>NH ⁺		
	3		Ar	-OH		>NH ⁺		
	3		Ar	-OH		>NH ⁺		
metoprolol	3		Ar	-OH		>NH ⁺		
	3		Ar	-OH		>NH ⁺		
	3		Ar	-OH		>NH ⁺		
	3		Ar	-OH		>NH ⁺		
	3		Ar	-OH		>NH ⁺		

^a H₁ and H₂, hydrophobic centers; A₁, A₂, and A_D, HB acceptors; D_A, HB donor (see Figure 1 for symbols of atoms and functional groups that appear as pharmacophore points). ^b A₂: >N₋₍₃₎ → 1; -OH₍₂₎ → 2; =O₍₂₎ → 3.

forms were reproduced and no participation of the >NH₋₍₂₎ atom was recorded. As seen from Table 6B, the ionized nitrogen is mostly the observed D_A point, but also the hydrogen atoms in the hydroxy groups were occasionally involved (vinblastine, quinidine). The patterns of the protonated norverapamil resembled fully those of the protonated verapamil, and ketoconazole was not charged at physiological pH (pK_a = 5.4, Table 1); therefore, the overlays with these drugs were not included in Table 6B. It should be noted that the A₁ point appeared in neither of the neutral forms of quinidine and quinine, although several runs were performed with different GASP parameters to increase

the conformational variety. In the ionized forms, however, A₁ was identified as the hydroxyl oxygen (Figure 2). In general, the topology of the protonated forms resembled that of the neutral ones but with the D_A point involved instead of the A_D one.

In summary, the results presented in Table 6 demonstrate that the most active drugs, such as vinblastine, rhodamine 123, verapamil, haloperidol, and ketoconazole, have four to six functional groups that can be involved in hydrophobic and HB interactions with the receptor and also several pharmacophore patterns possibly corresponding to different binding modes. The less active compounds (omeprazole and quinidine) have less

Table 7. Pharmacophore Patterns of MDR Drugs with ATPase Effect Identified in Overlays on Neutral (A) and Protonated (B) Forms with Vinblastine^a

(A) On Neutral Forms with Vinblastine								
compound	<i>n</i>	pharmacophore points						<i>D_A</i>
		<i>H</i> ₁	<i>H</i> ₂	<i>A</i> ₁	<i>A</i> ₂	<i>A_D</i>	<i>D_A</i>	
vinblastine	6	Ar1	Ar2	=O ₍₁₎	-OH ₍₂₎	-OH ₍₁₎	-OH ₍₁₎	
reserpine	4	Ar		=O ₍₁₎	=O ₍₂₎ ^b	>N-		
tamoxifen	3	Ar3	Ar1			>N-		
	3	Ar1	Ar2		>N-			
amiodarone	4	Ar1	Ar2	=O	>N-			
propafenone	5	Ar1	Ar2	=O				
	4	Ar1	Ar2			>NH		>NH
	4	Ar2	Ar1			-OH		-OH
	4	Ar2	Ar1			-OH		>NH
	4	Ar2	Ar1			>NH		>NH
	4	Ar2	Ar1			-OH		-OH
trifluoperazine	3	Ar2	Ar1			>N ⁻⁽¹⁾		
chlorpromazine	3	Ar2	Ar1			>N-		
triflupromazine	3	Ar2	Ar1			>N ⁻⁽¹⁾		

(B) On Protonated Forms with Vinblastine								
compound	<i>n</i>	pharmacophore points						<i>D_A</i>
		<i>H</i> ₁	<i>H</i> ₂	<i>A</i> ₁	<i>A</i> ₂	<i>A_D</i>	<i>D_A</i>	
vinblastine	6	Ar1	Ar2	=O ₍₁₎	-OH ₍₂₎	-OH ₍₁₎	>NH ⁻⁽¹⁾⁺	-OH ₍₁₎
reserpine	4	Ar		=O ₍₁₎	=O ₍₂₎			>NH ⁺
tamoxifen	3	Ar3	Ar1					>NH ⁺
amiodarone	4	Ar1	Ar2	=O				>NH ⁺ ^c
propafenone	5	Ar1	Ar2	=O		-OH		>NH ⁺
	4	Ar1	Ar2	=O			>NH ⁺	
	4	Ar1	Ar2	=O			>NH ⁺	
	4	Ar2	Ar1	=O			>NH ⁺	
trifluoperazine	4	Ar2	Ar1			>N ⁻⁽¹⁾		>NH ⁺
	3	Ar2	Ar1				>NH ⁻⁽¹⁾⁺	>NH ⁻⁽²⁾⁺
chlorpromazine	3	Ar2	Ar1				>NH ⁺	
triflupromazine	3	Ar2	Ar1				>NH ⁺	

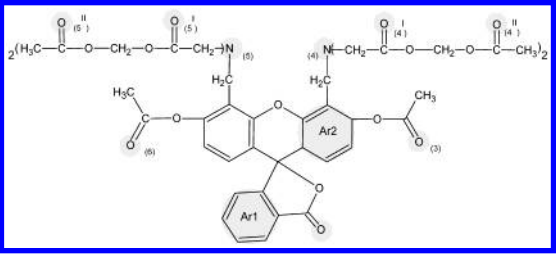
^a *H*₁ and *H*₂, hydrophobic centers; *A*₁, *A*₂, and *A_D*, HB acceptors; *D_A*, HB donor (see Figure 1 for symbols of atoms and functional groups that appear as pharmacophore points). ^b Overlaid occasionally on =O₍₃₎ of vinblastine. ^c Overlaid on -OH₍₂₎ of vinblastine.

pharmacophore patterns with three and four points involved. Finally, drugs such as pafenolol, quinine, propranolol, and metoprolol produce two and three pharmacophore patterns with three pharmacophore points involved. Thus, the following general tendency can be outlined: the more active the drug, the more pharmacophore points are simultaneously occupied and the more pharmacophore patterns (binding modes) are observed.

P-gp Drugs (ATPase Activity Effect). In Table 7A the pharmacophore patterns of several more compounds with high *K*₁ values for ATPase activity effect (Table 1) are presented including reserpine, tamoxifen, amiodarone, propafenone, trifluoperazine, chlorpromazine, and triflupromazine. In general, the obtained patterns confirm participation of the main pharmacophore points identified above, namely, *H*₁, *H*₂, *A*₁, *A_D*, *A*₂, and *D_A*. The oxygen atom of the -OH₍₂₎ group of vinblastine was mostly involved as the *A*₂ point, but =O₍₃₎ was also occasionally overlaid. The regularity between the number of the points and patterns, on one hand, and the level of ATPase activity effect, on the other hand, was not so clearly outlined as in case of the binding assay data. For example, tamoxifen had two patterns that involved three points only, but its *K*₁ value was the lowest in the set and equal to that of reserpine. Interestingly, tamoxifen was found as an outlier in the structure-activity study of the same set processed with the MolSurf program.²⁴ Amiodarone and propafenone produced patterns with four and five points involved but had higher *K*₁ compared to reserpine and tamoxifen.

Indeed, it is unknown whether all these drugs affect ATPase activity by the same interaction site. It is not clear as well what effect ATPase activity has on the drug interaction with the protein; it has been reported that the drug binding sites on P-gp are altered by ATP binding.²⁵ In general, there is no direct evidence for a correlation between inhibition of the P-gp-mediated drug transport and the drug-stimulated ATPase activity.²⁶ We studied the correlation between the log values of *K*₁₁ and *K*₁ (Table 1) for all of the drugs with measured effects in both test systems and obtained a significant correlation for a set involving five of them: vinblastine, verapamil, chlorpromazine, quinidine, and propranolol (*R*² = 0.86, *p* = 0.02). For these compounds, the regularity observed for the verapamil binding data followed the same tendency: the lower the *K*₁, the more pharmacophore points and pharmacophore patterns observed. Chlorpromazine was the only drug in the binding assay data that deviated from the observed regularity between the level of affinity and the number of obtained pharmacophore points and patterns. It showed one pattern with three points only (*H*₁, *H*₂, and *A_D*, Table 7) but had *K*₁₁ slightly higher than that of verapamil (0.6 μM, Table 1). Thus, either the *K*₁₁ value of chlorpromazine might be incorrect or other unknown reasons may be responsible for this high binding affinity. At the same time, chlorpromazine showed much weaker ATPase activity effect compared to verapamil (Table 1).

The charged forms of the drugs were also studied overlaid separately on the two monoprotonated forms

Table 8. Pharmacophore Points of Calcein-am Identified in Overlays on Vinblastine


pharmacophore point's type	compound's atom or group	
	vinblastine (template)	calcein
H ₁	Ar1	Ar1
H ₂	Ar2	Ar2
A ₁	=O ₍₁₎	=O, =O ₍₄₎ ^{II} , =O ₍₅₎ ^{II}
A _D	-OH ₍₁₎ , >N ⁻ ₍₁₎	>N ⁻ ₍₅₎ , =O ₍₅₎ ^I , =O ₍₅₎ ^{II} , =O ₍₆₎
D _A ^a	-OH ₍₁₎ , >NH ⁺ ₍₁₎	>NH ⁺ ₍₅₎
acceptor ^b	=O ₍₁₎ , =O ₍₂₎ , -OH ₍₂₎	=O ₍₃₎ , =O ₍₄₎ ^I , =O ₍₄₎ ^{II} , =O ₍₅₎ ^{II}

^a Observed in the protonated forms only. ^b One to four points.

of vinblastine. Again, no participation of the protonated >N⁻₍₂₎ was observed; therefore, only the results with the >N⁻₍₁₎ were reported (Table 7B). In general, the protonated forms resemble the topology of the neutral ones: the hydrogens of the protonated nitrogens are overlaid either on the hydroxy group -OH₍₁₎ as in the neutral forms (reserpine, tamoxifen, propafenone) or on >NH⁺₍₁₎ of vinblastine (propafenone, phenothiazines). Although according to the apparent pK_a, trifluoperazine (Figure 1) is >N⁻₍₂₎ protonated at physiological pH, the single value of >N⁻₍₁₎ also suggests the possible existence of its >NH⁺₍₁₎ form (Table 1). Therefore, the two monoprotonated forms of trifluoperazine were studied. The drug showed two patterns, one of them involving both nitrogens: >N⁻₍₁₎ acting as an acceptor and >NH⁺₍₂₎ acting as a donor. Thus, the presence of two tertiary nitrogens suggests more flexible behavior of perazine-type phenothiazines that, in general, show higher MDR reversing activity compared to the promazine-type drugs.^{27,28}

Calcein-am. Although no calcein-am binding data on the verapamil binding site of P-gp were available, the possible pharmacophore patterns of this widely recognized P-gp substrate¹⁶ were also investigated. The results of the overlays on vinblastine are summarized in Table 8. For simplicity, the bis(*N,N*-bis(carboxymethyl)aminomethyl) groups were not presented separately. Correspondingly, the same codes for the symmetrical carbonyl oxygen atoms in both chains of the tertiary nitrogens >N⁻₍₄₎ and >N⁻₍₅₎ were used. As seen from the table, the pharmacophore points H₁, H₂, A₁, and A_D were identified again. A very good coincidence was observed between the corresponding virtual receptor points of calcein-am and verapamil in their overlays on vinblastine (not shown). The receptor points corresponding to H₁, H₂, and A₁ were fully overlapped, and those corresponding to A_D were very closely located; the distances between the A_D receptor points of calcein-am (A_D = >N⁻₍₅₎, Table 8) and verapamil (A_D = >N⁻ or A_D = ≡N) were respectively 0.5 and 0.8 Å. Similarly to verapamil, the D_A point appeared only in the protonated forms. Several more HB acceptor points were additionally identified overlaying the oxygen atoms of the hydroxy and ester groups in the second ring system of vinblastine with those of the third and fourth position

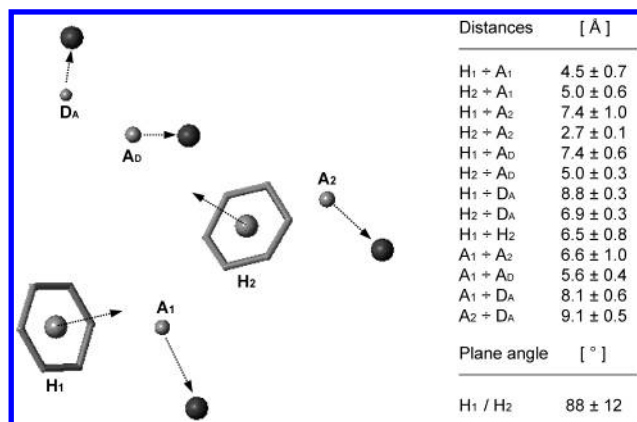


Figure 4. General pharmacophore pattern of drugs at the verapamil binding site of P-gp. H₁ and H₂ are hydrophobic points (shown as balls) located around the centers of the aromatic rings. A₁, A₂, and A_D are HB acceptor points. D_A is a HB donor point. The complementary HB donor and acceptor points of the receptor are presented also as balls at a distance of about 2.9 Å from the acceptor or donor atom of the drug in the direction of the lone pair or hydrogen. The arrows show directions of the hydrophobic and HB interactions. The values of distances between the pharmacophore points and of the angle between the aromatic planes are the average ± SD of the first several overlays with the highest fitness scores of vinblastine (on rhodamine 123), rhodamine 123 (on vinblastine), and *S*- and *R*-verapamil (on vinblastine).

substituents of calcein-am (Table 8). In neither of the alignments, >N⁻₍₃₎ of vinblastine appeared as an acceptor; however, =O₍₂₎, =O₍₃₎, and -OH₍₂₎ did (Table 8). It should be noted that calcein-am was the only drug among all studied ones that involved simultaneously more than one acceptor point (up to four) in this part of the vinblastine structure. Whether there is a single A₂ or more acceptor points in this part of the verapamil binding site cannot be decided yet. Moreover, calcein-am is not proved yet to bind to the investigated binding site of P-gp. It is possible also that the additional acceptor points are artifacts; the presence of more functional groups in calcein-am and conformational flexibility of the substituents containing these groups allow a large variety of overlays. A total of 20 alignments were also obtained with the neutral vinblastine (Vnbl-1) as a target and calcein-am as a template molecule (the global minimum conformer of calcein-am obtained by simulated annealing was used as a template, data not shown). Again, the main points were H₁, H₂, A₁, and A_D, confirming in this way their potential role in the pharmacophore pattern of P-gp drugs.

Figure 4 represents the general pharmacophore model of P-gp-related drugs at the verapamil binding site of the protein. The distances between the main pharmacophore points and the plane angle are the average of the highest fitness score overlays of the neutral forms of vinblastine, rhodamine 123, and both enantiomers of verapamil. As seen from the figure, the two hydrophobic planes are about orthogonally situated in the space and the main pharmacophore points H₁, H₂, A₁, and A_D in the pairs H₁-A₁, H₂-A₁, H₂-A_D, and A₁-A_D are separated by a regular step of about 5 Å.

Discussion

The question that arises first is how reasonable are the identified pharmacophore points. The hydrophobic

centers H₁ and H₂ are certainly involved because they appear as pharmacophore points in the alignments of almost all drugs and constantly in those of the most active ones. Two aromatic rings as prerequisites for interaction with P-gp have also been proposed by a number of authors (see ref 8 and references therein). Our modeling studies outlined hydrophobic fields as a key 3D property of the MDR modulators,^{29–31} suggesting the importance of the space-directed hydrophobicity for the drug MDR reversal activity.

The HB acceptor interactions are also considered as an important component in the protein binding of the MDR drugs. The predominant role of HB acceptor over HB donor interactions is reported in many studies.^{5–7,24,32} In this study three HB acceptor points are identified: A₁, A₂, and A_D. The A₁ point appears as a stable pharmacophore element in both neutral and protonated drugs. Together with the hydrophobic centers, it composes the most often observed combination of pharmacophore points that is a constant part in the patterns of the active drugs (Tables 2 and 4–6). Thus, H₁, H₂, and A₁ are likely to form the conservative element in the pharmacophore pattern of the P-gp drugs.

The A₂ point was identified in vinblastine, rhodamine 123, verapamil, haloperidol, ketoconazole, quinidine, quinine, and metoprolol but also in reserpine, tamoxifen, and amiodarone. In vinblastine, in addition to >N₍₃₎, several more functional groups, namely, –OH₍₂₎, =O₍₂₎, =O₍₃₎, were involved in the same function. These atoms were closely located and belonged to conformationally flexible substituents (Figure 1), and every time, only one of them appeared as an acceptor point. These facts imply that an HB interaction (HB acceptor for the ligand and HB donor for P-gp) can certainly take place in this part of the space and that A₂ might be a flexible pharmacophore point which position cannot be exactly defined. Our results do not allow to state firmly that A₂ is the only HB acceptor point, although it appears as a single point in this part of the overlay of all studied drugs except for calcein-am. As already mentioned, further studies should show whether additional HB acceptor points as identified in the overlays with calcein-am are really involved. We compared the HB acceptor capacities (Ca) of those vinblastine atoms that could act as A₂ using the program HYBOT³³: 1.27 (>N₍₃₎), 1.52 (oxygen in –OH₍₂₎), 1.43 (=O₍₃₎), and 1.19 (=O₍₂₎). The Ca values suggest compatible HB acceptor affinities of these atoms with some preferences to the hydroxyl oxygen but do not answer the question about the number of the HB acceptor points possibly involved. On the basis of the presented results, however, one can conclude that at least one HB acceptor point in this part is certainly involved in interaction with the verapamil binding site of P-gp.

The A_D point was first identified in the overlays with verapamil and appeared subsequently in the patterns of a number of P-gp drugs. As already suggested, although no A_D was identified in the overlays between vinblastine and rhodamine 123, this did not exclude the possibility of rhodamine 123 interacting by such a point too. In the runs of verapamil on rhodamine 123, it was observed in overlays between the =NH of rhodamine 123 and the >N₍₁₎ of verapamil but in a direction opposite to that obtained with verapamil on vinblastine.

This can be explained with the planar geometry of =NH, in which the lone pair of the nitrogen atom pointed in an opposite direction. Obviously, the =NH group may play a dual role in rhodamine 123 similarly to the –OH₍₁₎ group in vinblastine. The reason A_D is not to be identified in the overlays of vinblastine on rhodamine 123 might be related to the less conformational flexibility of vinblastine as a target compared to verapamil. Similarly to A₂, different atoms belonging to closely located and conformationally flexible parts in the same structure were identified as A_D, suggesting that it can be a flexible pharmacophore point, e.g., vinblastine (–OH₍₁₎ and >N₍₁₎), quinidine (>N₍₁₎ and –OH), propranolol (>NH and –OH).

The D_A point is directly related to the A_D one. The used codes reflect the dual role of some atoms and groups in the investigated structures, e.g., >N₍₁₎ and >NH⁺, –OH, =NH, >NH. The tertiary nitrogen appeared as a common structural element in almost all P-gp drugs. Depending on the interacting form (neutral or protonated) of the drug (see Discussion below), this atom can act as an A_D or D_A point. However, in a number of compounds, hydrogen atoms different from the proton of the charged nitrogen were also found to perform the D_A function in both the neutral and protonated forms (vinblastine (–OH₍₁₎), rhodamine 123 (=NH), quinidine (–OH), pafenolol (–OH), propranolol (>NH and –OH), propafenone (>NH and –OH) (Tables 6 and 7). In some overlays both A_D and D_A appeared (vinblastine, quinidine, propranolol, propafenone) in the same pattern. The related functions of A_D and D_A suggest that both points can simultaneously be involved in interactions with the protein, providing there is an appropriate group or groups in the receptor too, e.g., –OH in the serine residues of P-gp shown to affect its substrate specificity.³⁴

In close relation to the relevance of the identified pharmacophore points is the interacting form (neutral/ionized) of the studied compounds. It is known that the P-gp-related drugs are lipophilic and mostly basic compounds that are protonated at physiological pH. Most of the currently proposed models of P-gp functioning⁸ suggest that the drug binds to the protein in the membrane environment, presuming in this way the possibility for interaction of the protein with the neutral form of the drug. Estimating the importance of the nitrogen atom in MDR modulators of propafenone-related amines, anilines, and amides, Ecker et al. suggested that the interaction of the nitrogen with P-gp is nonionic.³⁵ Consistent with this suggestion, they showed recently that photoactivatable propafenone-type ligands labeled preferentially fragments assigned to the transmembrane domains of P-gp.³⁶ Fezard et al.³⁷ demonstrated that the presence of the protonable basic nitrogen of anthracycline facilitated the processing of these compounds by the MDR efflux system, but the positive charge was not a necessary requirement for P-gp recognition. However, in inside-out vesicles, the permanently charged derivative of dextriguldipine³⁸ and quaternary propafenone analogues³⁹ were identified as P-gp substrates. Thus, whether the drug binds to P-gp in its ionized form or the neutral form is the interacting one is still a debatable question. The interacting forms of the P-gp drugs may depend on the location of the

binding sites on the protein that, in case of P-gp, is yet to be elucidated. The case becomes even more complicated because the same binding site could adopt high- and low-affinity conformation.⁴⁰ The binding data used in this study were successfully approximated by the one- and two-affinity model; however, nothing definitive was reported about the location and the conformation of the verapamil binding site of P-gp.¹⁴ Subsequently, no drug form could be given any preferences. In the case of the ATPase activity effect,¹⁰ both drug forms are also possible; because the cytosolic domains of P-gp are responsible for ATP binding and hydrolysis, the drug can exist in a neutral and/or charged form depending on its pK_a . Thus, one can only speculate about the proper interacting form of the studied drugs. The results of this study suggest participation of several HB acceptor and one HB donor pharmacophore points simultaneously in the pharmacophore pattern for the verapamil binding site. As already discussed, the HB donor point D_A was observed not only in the protonated but also in the neutral form of a number of compounds. At the same time, drugs that are predominantly uncharged at physiological pH possess strong binding affinity, e.g., rhodamine 123 and ketoconazole (Table 1). Thus, the protonation might not be an obligatory requirement for binding to the verapamil binding site, but the HB donor interaction is not excluded for the neutral form. At the same time, the possibility of the protonated form to be a functional one (with the proton of the charged nitrogen acting as D_A) could not be rejected. Our results show that the neutral and protonated pharmacophore patterns follow similar topology, suggesting similar geometry of the corresponding binding site or sites on the protein.

Till now several pharmacophore patterns have been reported for MDR-related drugs. In the series of quinolines, Suzuki et al.⁵ stress the angle between the planes of the aromatic rings as an essential feature of the highly active MDR modulators. Considering only aryl rings in either three-cyclic systems or connected by a single $-CH-$ group, the value of about 100° (80° deviation from planarity) was reported for the most active representatives. This value is close to our finding (the average plane angle between the aromatic rings is 88° ; Figure 4). In the same study, a distance of at least 5 Å between the aromatic centroid (the middle point of the line connecting the centroids of the aryl rings) and the basic nitrogen was recorded. In a series of podophyllotoxins,⁶ where no basic nitrogen was present, a distance of 5 Å between the hydrophobic center and the HB acceptor group was also reported as a prerequisite for P-gp recognition. Seelig and Landwojtowich^{7,41} reported on two types of patterns formed by electron donor groups (oxygen, tertiary amino group, cyano group, halides, sulfides, or π -electron systems), at least one with 2.5 ± 0.3 Å and a second with 4.6 ± 0.6 Å spatial separation, as necessary recognition elements for P-gp binding. In our model, an average distance of 5 Å was observed between H_1 and A_1 (4.5 ± 0.7 Å), H_2 and A_1 (5.0 ± 0.6 Å), H_2 and A_D (5.0 ± 0.3 Å), and A_1 and A_D (5.6 ± 0.4 Å) and a distance 2.7 ± 0.1 Å between H_2 and A_2 , in agreement with published results. Additionally, higher distances were recorded between some HB acceptor points, e.g., H_1 and H_2 (6.5 ± 0.8 Å), A_1 and A_2 (6.6 ± 1.0 Å), and H_1 and A_2 (7.4 ± 1.0 Å) (Figure 4).

Very recently Penzoti et al.⁴² reported a computational ensemble pharmacophore model for classification of P-gp drugs as substrates and nonsubstrates using the Seelig study⁷ as a starting point. The top scoring pharmacophore in the ensemble consisted of two hydrophobes: one HB acceptor and one HB donor. The distances between the HB acceptors reproduced those in the pattern of Seelig.⁷ These models, as mentioned in the Introduction, are based on data obtained from different cell lines, assays, and conditions and do not consider how molecules interact with P-gp and which binding site is involved. In the literature, clustering of P-gp drugs as substrates and nonsubstrates/inhibitors is done on either cytotoxicity/accumulation assays⁴³ or data on drugs known to be transported or not by P-gp⁴² and, therefore, do not account for a particular protein binding site. Our model relies on affinities to the same protein binding site and, thus, cannot differentiate between substrates and nonsubstrates in the above sense. Considering that the specific pharmacophore model should address the individual P-gp binding site, Ekins et al. proposed recently a number of pharmacophore models using diverse sets of inhibitors.⁴⁴ They derived also a model for the verapamil binding site of P-gp,⁴⁵ based on data of Neuhoﬀ et al.¹⁴ The model consisted of four features: two hydrophobic (aromatic rings and aliphatic chains), one HB acceptor, and one aromatic ring features. Although some of the most active drugs (vinblastine and rhodamine 123) reported to bind the same protein site¹¹ were not involved and the computational approach of Catalyst was applied, the obtained model agrees with ours in two hydrophobic regions and at one HB acceptor point as necessary elements for P-gp recognition. On the basis of a highly diverse set of drugs, our model contains more HB interaction points and, additionally, provides directions of the hydrophobic and HB interactions toward the virtual receptor sites. These results can direct, on one hand, the correct alignment of the drugs for subsequent 3D-QSAR studies and, on the other hand, can help the correct identification of the relevant P-gp amino acid residues responsible for the drug binding.

How realistic were the drug conformations obtained by GASP is another point of discussion. It should be stated in advance that in this study GASP was mainly used for identification of those structural features of the studied drugs that may represent potential elements of their P-gp-related pharmacophore patterns. Therefore, single structures were only analyzed in order to estimate how reasonable the geometries of the obtained conformations were. As shown in the examples of rhodamine 123 (Table 3), the geometrical characteristics related to the main pharmacophore points in the resulting GASP conformations were very close to those in the conformations identified as global minimum conformers. This implies that the obtained GASP conformations have energetically reasonable geometry. The analysis of the energy terms for some conformations indicated the presence of bad steric contacts. Because no full molecular mechanics potential is implemented in the GASP algorithm, a final optimization of the generated structures is considered to be appropriate.⁴⁶ Indeed, to address the problem of minimization distortion, an

increase in the relative weighting of the vdW energy term and/or selection of the option to include the torsional energy term is recommended.⁴⁶ Considering that the purpose of this study was identification of the common pharmacophore elements of diverse MDR-related drugs, we did not explore these possibilities. However, it was shown that the identified conformations of the most active drugs resembled very closely their global minimum conformers.

The key point of the work is the relation of the featured pharmacophore points to the reported affinity values and subsequently to the reasons that can explain the high structural variety of the studied drugs. Although no QSARs are derived, activities of the studied drugs (Table 1) can be qualitatively related to the number and type of the occupied pharmacophore points (Table 2 and 4–6). In general, the binding affinity of the drugs depends on the presence of relevant functional groups in an appropriate spatial arrangement that can meet the structural requirements for recognition by P-gp. Obviously, the compounds with high binding affinity meet better the structural requirements for P-gp recognition than those with lower affinity. The active drugs contain the highest number of functional groups able to perform hydrophobic and HB acceptor interactions and, at the same time, have the highest number of pharmacophore patterns or, in other words, binding modes. It should be noted, however, that we also observed an exception in the case of tiapamil. Although this compound resembles the pharmacophore patterns of verapamil (data not shown), its K_{i1} is 12.02 μM .¹⁴ Obviously, additional factors can play a role, e.g., total lipophilicity (ClogP = 0.843 versus 3.79 of verapamil⁴⁷). Thus, the general tendency is the more active the drug, the more pharmacophore points are simultaneously involved in interactions and/or the more pharmacophore patterns (binding modes) are possible.

Our results suggest that the verapamil binding site might be part of a large binding pocket with discrete domains of specificity that correspond to different pharmacophore points. The binding of the drugs to the protein can take place through a wide interaction surface on P-gp, and the drugs, depending on their functional groups and conformations, can interact with different receptor points. Moreover, this large site certainly undergoes some conformational changes just like the flexible P-gp drugs can, so both the protein and the drug adopt each other in the best way depending on their hydrophobic and HB interaction capabilities, a fact suggested for other MDR transporters.⁴⁸

Conclusions

The pharmacophore patterns of P-glycoprotein drugs proposed till now either relate to a strongly homologous series of compounds or utilize structurally diverse drugs tested as P-gp substrates and inhibitors in different test systems and different tumor cell lines. In this study, a general pharmacophore model of P-gp drugs is proposed that is based on binding data of a highly diverse data set and relates to a defined binding site of the protein. The model is derived from structurally different compounds that bind to the verapamil binding site of P-gp. A number of drugs were studied including anticancer agents, calcium channel blockers,

neuroleptic, antifungal, and antimalarial drugs, proton pump inhibitors, and their analogues and stereoisomers. The genetic algorithm similarity program GASP was applied for molecular alignment and pharmacophore definition. The pharmacophore points were identified by overlays of the most active and rigid compounds in the set. A general pharmacophore pattern was proposed for the verapamil binding site of P-gp that involved two hydrophobic planes H_1 and H_2 , three hydrogen bond (HB) acceptors A_1 , A_2 , and A_D , and one HB donor D_A . The angle between the hydrophobic planes and distances between the points were calculated as an average of those in the most active compounds: vinblastine, rhodamine 123, and verapamil enantiomers. The angle between the hydrophobic planes was about 90° , and the distances H_1-A_1 , H_2-A_1 , H_2-A_D , and A_1-A_D were about 5 Å. The directions of the hydrophobic and HB interactions were defined as virtual receptor sites. The specific interaction points and pharmacophore patterns of various drugs were derived, and different binding modes were suggested for some of them. The same pharmacophore patterns were identified for enantiomers in agreement with their binding affinity. Additionally several more drugs known as P-gp substrates and inhibitors including the widely used fluorescent probe calcein-am were investigated for the presence of functional groups corresponding to the identified pharmacophore points. It was demonstrated that the binding affinity of the P-gp-related drugs depended on the number of the pharmacophore points simultaneously involved in the interaction with the protein. On the basis of the obtained results, a hypothesis is proposed to explain the broad structural variety of the P-gp substrates and inhibitors: (i) the verapamil binding site of P-gp has several points that can participate in hydrophobic and HB interactions; (ii) different drugs can interact with different receptor points in different binding modes.

Experimental Section

Structure Preparation. Vinblastine. The X-ray structure of vinblastine was taken from Cambridge Crystallographic Database (code SIMLAB).⁴⁹ The structure was first minimized by the Tripos force field (Powell method, 0.05 kcal mol⁻¹ Å⁻¹ gradient, no charges) and then optimized by the semiempirical quantum chemistry method AM1 (full optimization using the key words "Precise" and XYZ) as implemented in MOPAC 7.0.⁵⁰ The resulting conformation served as a starting point for identification of the energy minimum conformers of vinblastine. Two techniques were applied: systematic search and simulated annealing.²⁰ In the systematic search, the rotatable bonds between the two ring systems of vinblastine and the first ester group connected to it (marked by t_1 and t_2 in Figure 1) were simultaneously varied with increment 30° using the Tripos force field. To avoid a loss of conformations, the vdW scale factors for the bump check were set to 0.7 (general), 0.6 (1–4), and 0.5 (H-bond). The local minimum conformers within the energy range of 20 kcal/mol above the global energy minimum obtained were selected and subsequently minimized (Powell method, 0.05 kcal mol⁻¹ Å⁻¹ gradient, Gasteiger–Hückel charges). Four clusters were identified after minimization within an energy interval of 5 kcal mol⁻¹ Å⁻¹ that differed by the mutual orientation of the two ring systems and the first ester group. The conformer with the lowest energy in each cluster was selected (coded from Vnbl-1 to Vnbl-4, respectively) for subsequent use as a template in the GASP runs. The results are summarized in Table 9. As seen from the table,

Table 9. Vinblastine Conformers Used in the GASP Runs^a

conformation	torsions, ^b deg		Ar1/Ar2 plane angle, ^a deg	E_{\min} , ^c kcal mol ⁻¹ Å ⁻¹
	t_1	t_2		
Vnbl-1	55.3	13.4	79.6	58.8
Vnbl-2	58.4	-152.6	79.0	59.7
Vnbl-3	160.2	122.8	75.5	61.3
Vnbl-4	161.3	-47.2	74.7	62.8
Vnbl-SA	50.5	14.1	79.6	56.8

^a See Figure 1 for designations t_1 , t_2 , Ar1, and Ar2. ^b Measured in the range -180° to 180°. ^c Tripos force field, 0.05 kcal mol⁻¹ Å⁻¹ gradient, no charges.

Vnbl-1 and Vnbl-2, on one hand, and Vnbl-3 and Vnbl-4, on the other hand, have close t_1 but opposite t_2 values. Vnbl-1 has the lowest energy E_{\min} . To check on the validity of the obtained conformer, a simulated annealing was also performed with the following settings: 100 cycles, 1000 K initial temperature for heating for 2000 fs equilibration, 0 K target temperature for 10000 fs annealing time, and exponential annealing function. The plot of energy versus time of the obtained 100 local minima showed the 3 lowest energy conformers within 0.4 kcal/mol above the global minimum. The conformer with the lowest energy after minimization (Vnbl-SA, Table 9) was compared to that identified from a systematic search (Vnbl-1). As seen from the table, both conformers have almost equal torsions t_1 and t_2 and Ar1/Ar2 plane angles. Additionally the correspondence between the main functional groups of Vnbl-1 and Vnbl-SA was checked by the rms fit. An excellent correspondence was observed; the rms value was 0.049 by fitting the centroids of the aromatic rings, =O₍₁₎, >N₍₋₁₎, >N₍₋₃₎, and -OH₍₁₎ (Figure 1). Vnbl-1 and Vnbl-SA were further optimized by AM1 (full optimization using the key words "Precise" and XYZ). Vnbl-SA had a heat of formation of -224.2 kcal compared to -238.4 kcal of Vnbl-1. Thus, Vnbl-1 was selected as the global minimum conformer of vinblastine.

Rhodamine 123. The X-ray structure of bis(rhodamine123) tetrachloroplatinum tetrahydrate was taken from ref 49 (code FACKEZ), modified to rhodamine 123, and subsequently optimized. Similarly to vinblastine, a systematic search was performed simultaneously on the rotatable bonds between both ring systems and the ester group (shown by t_1 and t_2 in Figure 1). Two global minimum conformers of equal energy were identified with an opposite orientation of the acidic ring toward the three-cyclic ring system and the ester groups, respectively: -67.9° and 171.7° (R123-1) and 67.5° and -171.7° (R123-2) (Table 3).

Verapamil and Its Derivatives. The X-ray structure of *R*-verapamil was found in ref 49 (code CURHOM). The structure was folded with an angle of 68.9° between the planes of the phenyl rings. The conformation of verapamil was determined as well in acetonitrile using two-dimensional ¹H NMR and molecular modeling.⁵¹ This structure differed significantly from the X-ray one, being much more extended with aromatic rings located apart from each other. The structure of verapamil was built according to the torsions published in ref 51. The resulting structure was the *S*-enantiomer. The *R*-enantiomer was built from the *S*-one. Both conformers showed the same heat of formation (-88.8 kcal/mol) after AM1 optimization (full, with the key "Precise"). The verapamil derivatives were built from the corresponding enantiomers of verapamil, and their heats of formations were compared in order to ensure that the right enantiomer forms were used.

Other Compounds. Most of the structures of the other compounds were built from their X-ray structures.⁴⁹ Quinidine ((8*S*,9*R*)-6'-methoxy-9-chinchonalol) and quinine (8*R*,9*S*)-6'-methoxy-9-chinchonalol) were also obtained from their X-ray structures. Enantiomers of the other drugs (norverapamil, omeprazole, pafenolol, propranolol, metoprolol, propafenone) were built in a way similar to that of the verapamil enantiomers. The structure of calcein-am was built in SYBYL, and the global minimum conformer as found by simulated annealing was used in the GASP runs. The structures of chlorpromazine, trifluoperazine, trifluopromazine, and propafenone were taken from our previous CoMFA models.^{29,30}

The protonated forms of the drugs were built from their neutral forms considering the protonation state at physiological pH according to the reported p*K*_a values (Table 1). Two monoprotonated forms were generated for drugs such as vinblastine and trifluoperazine with two tertiary nitrogens, with close p*K*_a values (Table 1), respectively on N₍₁₎ and N₍₂₎ (Figure 1).

Prior to the GASP runs, all structures were assigned Gasteiger-Hückel charges and minimized using the Tripos force field (Powell method, 0.05 kcal mol⁻¹ Å⁻¹ convergence criterion).

GASP Settings. The GASP parameters were set to the following default values: population size 100; selection pressure 1.1; maximum number of operations 60 000; operation increment 6500; fitness increment 0.01; point cross weight 95.0; allele mutate weight 95.0; full mutation weight 0.0; full crossweight 0.0; internal vdW energy coefficient 0.05; HB weight coefficient 750; vdW contact cutoff 0.8. Additionally several control runs were performed increasing the population size to 125 and the allele mutate weight to 96.0 in order to increase the diversity of conformations considered. No increase in conformational diversity was observed.

Acknowledgment. The authors thank the Alexander von Humboldt Foundation (Grant V-8131-BUL/1021057) for the main financial support and the National Science Fund of Bulgaria (Grant L-910).

References

- Ambudkar, S. V.; Dey, S.; Hrycyna, C. A.; Ramachandra, M.; Pastan, I.; Gottesman, M. Biochemical, Cellular, and Pharmacological Aspects of the Multidrug Transporter. *Annu. Rev. Pharmacol. Toxicol.* **1999**, *39*, 361-398.
- Pearce, H. L.; Safa, A. R.; Bach, N. J.; Winter, M. A.; Cirtain, M. C.; Beck, W. T. Essential Features of the P-Glycoprotein Pharmacophore As Defined by a Series of Reserpine Analogs That Modulate Multidrug Resistance. *Proc. Natl. Acad. Sci. U.S.A.* **1989**, *86*, 5128-5132.
- Pearce, H. L.; Winter, M. A.; Beck, W. T. Structural Characteristics of Compounds That Modulate P-Glycoprotein-Associated Multidrug Resistance. *Adv. Enzyme Regul.* **1990**, *30*, 357-373.
- Hait, W. N.; Aftab, D. Rational Design and Pre-clinical Pharmacology of Drugs for Reversing Multidrug Resistance. *Biochem. Pharmacol.* **1992**, *43*, 103-107.
- Suzuki, T.; Fukazawa, N.; San-nohe, K. Structure-Activity Relationship of Newly Synthesized Quinoline Derivatives for Reversal of Multidrug Resistance in Cancer. *J. Med. Chem.* **1997**, *40*, 2047-2052.
- Etievant, C.; Schambel, P.; Guminski, Y.; Barret, J.-M.; Imbert, T.; Hill, B. T. Requirements for P-Glycoprotein Recognition Based on Structure-Activity Relationships in the Podophylotoxin Series. *Anti-Cancer Drug Des.* **1998**, *13*, 317-336.
- Seelig, A. A General Pattern for Substrate Recognition by P-Glycoprotein. *Eur. J. Biochem.* **1998**, *251*, 252-261.
- Wiese, M.; Pajeva, I. Structure-Activity Relationships of Multidrug Resistance Reversers. *Curr. Med. Chem.* **2001**, *8*, 685-713.
- Zamora, J. M.; Pearce, H. L.; Beck, W. T. Physical-Chemical Properties Shared by Compounds That Modulate Multidrug Resistance in Human Leukemic Cells. *Mol. Pharmacol.* **1998**, *33*, 454-462.
- Litman, T.; Zeuthen, T.; Skovsgaard, T.; Stein, W. D. Structure-Activity Relationships of P-Glycoprotein Interacting Drugs: Kinetic Characterization of Their Effects on ATPase Activity. *Biochim. Biophys. Acta* **1997**, *1361*, 159-168.
- Doeppenschmitt, S.; Spahn-Langguth, H.; Regard, C. G.; Langguth, P. Radioligand-Binding Assay Employing P-Glycoprotein-Overexpressing Cells: Testing Drug Affinities to the Secretory Intestinal Multidrug Transporter. *Pharm. Res.* **1998**, *15*, 1001-1006.
- Doeppenschmitt, S.; Langguth, P.; Regard, C. G.; Andersson, T. B.; Hilgendorf, C.; Spahn-Langguth, H. Characterization of Binding Properties to Human P-Glycoprotein: Development of a [³H]Verapamil Radioligand-Binding Assay. *J. Pharmacol. Exp. Ther.* **1999**, *288*, 348-357.
- Doeppenschmitt, S.; Spahn-Langguth, H.; Regard, C. G.; Langguth, P. Role of P-Glycoprotein-Mediated Secretion in Absorptive Drug Permeability: An Approach Using Passive Membrane Permeability and Affinity to P-Glycoprotein. *J. Pharm. Sci.* **1999**, *88*, 1067-1072.

- (14) Neuheoff, S.; Langguth, P.; Dressler, C.; Andersson, T. B.; Regardh, C. G.; Spahn-Langguth, H. Affinities at the Verapamil Binding Site of MDR1-Encoded P-Glycoprotein: Drugs and Analogs, Stereoisomers and Metabolites. *Int. J. Clin. Pharm. Ther.* **2000**, *38*, 168–179.
- (15) Jones, G.; Willett, P.; Glen, R. C. A Genetic Algorithm for Flexible Molecular Overlay Pharmacophore Elucidation. *J. Comput.-Aided Mol. Des.* **1995**, *9*, 532–549.
- (16) Tiberghien, F.; Loo, F. Ranking of P-Glycoprotein Substrates and Inhibitors by a Calcein-am Fluorometry Screening Assay. *Anti-Cancer Drugs* **1996**, *7*, 568–578.
- (17) Martindale, W. *The Extra Pharmacopoeia/Martindale*, 30th ed.; Pharmaceutical Press: London, 1993.
- (18) Craig, P. N. Drug Compendium. In *Comprehensive Medicinal Chemistry*; Hansch, C., Sammes, P. G., Taylor, J. B., Eds.; Pergamon: Oxford, 1990; Vol. 6, pp 237–991.
- (19) Franke, U.; Munk, A.; Wiese, M. Ionization Constants and Distribution Coefficients of Phenothiazines and Calcium Channel Antagonists Determined by a pH-Metric Method and Correlation with Calculated Partition Coefficients. *J. Pharm. Sci.* **1999**, *88*, 89–95.
- (20) Sybyl, version 6.7; Tripos Inc., 1699 South Hanley Road, St. Louis, MO 63144-2917; October 2000.
- (21) URL: <http://www.acdlabs.com>. E-mail: robin.martin@acdlabs.com.
- (22) Safa, A. R. Photoaffinity Labeling of the Multidrug-Resistance-Related P-Glycoprotein with Photoactive Analogs of Verapamil. *Proc. Natl. Acad. Sci. U.S.A.* **1988**, *85*, 7187–7191.
- (23) van der Sandt, I. C. J.; Blom-Rosemalen, M. C. M.; de Boer, A. G.; Breimer, D. D. Specificity of Doxorubicin versus Rhodamine-123 in Assessing P-Glycoprotein Functionality in the LLC-PK1, LLC-PK1 MDR1 and Caco-2 Cell Lines. *Eur. J. Pharm. Sci.* **2000**, *11*, 207–214.
- (24) Österberg, T.; Norinder, U. Theoretical Calculation and Prediction of P-Glycoprotein Interacting Drugs Using MolSurf Parameterization and PLS Statistics. *Eur. J. Pharm. Sci.* **2000**, *10*, 295–303.
- (25) Martin, C.; Berridge, G.; Mistry, P.; Higgins, C.; Charlton, P.; Callaghan, R. Drug Binding Sites on P-Glycoprotein Are Altered by ATP Binding Prior to Nucleotide Hydrolysis. *Biochemistry* **2000**, *39*, 11901–11906.
- (26) Julien, M.; Kajiji, S.; Kaback, R. H.; Gros, P. Simple Purification of Highly Active Biotinylated P-Glycoprotein: Enantiomer-Specific Modulation of Drug-Stimulated ATPase Activity. *Biochemistry* **2000**, *39*, 75–85.
- (27) Ford, J. M.; Prozialeck, W. C.; Hait, W. N. Structural Features Determining Activity of Phenothiazines and Related Drugs for Inhibition of Cell Growth and Reversal of Multidrug Resistance. *Mol. Pharmacol.* **1989**, *35*, 105–115.
- (28) Ford, J. M.; Bruggemann, E. P.; Pastan, I.; Gottesman, M. M.; Hait, W. N. Cellular and Biochemical Characterization of Thioxanthenes for Reversal of Multidrug Resistance in Human and Murine Cell Lines. *Cancer Res.* **1990**, *50*, 1748–1756.
- (29) Pajeva, I. K.; Wiese, M. Molecular Modeling of Phenothiazines and Related Drugs as Multidrug Resistance Modifiers: A Comparative Molecular Field Analysis Study. *J. Med. Chem.* **1998**, *41*, 1815–1826.
- (30) Pajeva, I. K.; Wiese, M. A Comparative Molecular Field Analysis of Propafenone-Type Modulators of Cancer Multidrug Resistance. *Quant. Struct.-Act. Relat.* **1998**, *17*, 301–312.
- (31) Pajeva, I. K.; Wiese, M. Multidrug Resistance Related Drugs: Estimation of Hydrophobicity as a Space Directed Molecular Property. *C. R. Acad. Bulg. Sci.* **2001**, *54*, 81–84.
- (32) Pajeva, I. K.; Wiese, M. Human P-Glycoprotein Pseudoreceptor Modeling: 3D-QSAR Study of Thioxanthene Type Multidrug Resistance Modulators. *Quant. Struct.-Act. Relat.* **2001**, *20*, 130–138.
- (33) Raevsky, O. A. Quantification of Non-covalent Interaction on the basis of the Thermodynamic Hydrogen Bond Parameters. *J. Phys. Org. Chem.* **1997**, *10*, 405–413 (with special thanks to the help of Dr. K.-J. Schaper, Borstel Research Institute, Germany).
- (34) German, U. A. P-Glycoprotein-a Mediator of Multidrug Resistance in Tumour Cells. *Eur. J. Cancer* **1996**, *32A*, 927–944.
- (35) Ecker, G.; Huber, M.; Schmid, D.; Chiba, P. The Importance of a Nitrogen Atom in Modulators of Multidrug Resistance. *Mol. Pharmacol.* **1999**, *56*, 791–796.
- (36) Ecker, G. F.; Csaszar, E.; Kopp, S.; Plagens, B.; Holzer, W.; Ernst, W.; Chiba, P. Identification of Ligand-Binding Regions of P-Glycoprotein by Activated-Pharmacophore Photoaffinity Labeling and Matrix-Assisted Laser Desorption/Ionization-Time-Of-Flight Mass Spectrometry. *Mol. Pharmacol.* **2002**, *61*, 637–648.
- (37) Frezard, F.; Pereira-Maia, E.; Quidu, P.; Priebe, W.; Garnier-Suillerot, A. P-Glycoprotein preferentially effluxes anthracyclines containing free basic versus charged amine. *Eur. J. Biochem.* **2001**, *268*, 1561–1567.
- (38) Ferry, D.; Boer, R.; Callaghan, R.; Ulrich, W.-R. Localization of the 1,4-Dihydropyridine Drug Acceptor of P-Glycoprotein to a Cytoplasmic Domain Using a Permanently Charged Derivative *N*-Methyl Dextrinogulidipine. *Int. J. Clin. Pharmacol. Ther.* **2000**, *38*, 130–140.
- (39) Schmid, D.; Ecker, G.; Kopp, S.; Hitzler, M.; Chiba, P. Structure-Activity Relationship Studies of Propafenone Analogs Based on P-Glycoprotein ATPase Activity Measurements. *Biochem. Pharmacol.* **1999**, *58*, 1447–1456.
- (40) Martin, C.; Higgins, C. F.; Callaghan, R. The Vinblastine Binding Site Adopts High- and Low-Affinity Conformations during a Transport Cycle of P-Glycoprotein. *Biochemistry* **2001**, *40*, 15733–15742.
- (41) Seelig, A.; Landwojtowicz, E. Structure-Activity Relationship of P-Glycoprotein Substrates and Modifiers. *Eur. J. Pharm. Sci.* **2000**, *12*, 31–40.
- (42) Penzoti, J. E.; Lamb, M. L.; Evensen, E.; Grootenhuys, P. D. J. A Computational Ensemble Pharmacophore Model for Identifying Substrates of P-Glycoprotein. *J. Med. Chem.* **2002**, *45*, 1737–1740.
- (43) Scala, S.; Akhmed, N.; Rao, U. S.; Paull, K.; Lan, L.-B.; Dickstein, B.; Lee, J.-S.; Elgemeie, G. H.; Stein, W. D.; Bates, S. E. P-Glycoprotein Substrates and Antagonists Cluster into Two Distinct Groups. *Mol. Pharmacol.* **1997**, *51*, 1024–1033.
- (44) Ekins, S.; Kim, R. B.; Leake, B. F.; Dantzig, A. H.; Schuetz, E. G.; Lan, L.-B.; Yasuda, K.; Shepard, R. L.; Winter, M. A.; Schuetz, J. D.; Wikel, J. H.; Wrighton, S. A. *Mol. Pharmacol.* **2002**, *61*, 964–973.
- (45) Ekins, S.; Kim, R. B.; Leake, B. F.; Dantzig, A. H.; Schuetz, E. G.; Lan, L.-B.; Yasuda, K.; Shepard, R. L.; Winter, M. A.; Schuetz, J. D.; Wikel, J. H.; Wrighton, S. A. *Mol. Pharmacol.* **2002**, *61*, 974–981.
- (46) SYBYL/GASP Interface, *Ligand-Based Design Manual*, version 6.7; Tripos, Inc., 1699 South Hanley Road, St. Louis, MO 63144-2917; October 2000.
- (47) *ClogP for Windows*, version 1.0.0; BioByte Corp., 201 West 4th Street, Suite 204, Claremont, CA 91711; 1995.
- (48) Vazquez-Laslop, N.; Zheleznova, E. E.; Markham, P. N.; Brennan, R. G.; Neyfakh, A. A. Recognition of Multiple Drugs by a Single Protein: A Trivial Solution of an Old Paradox. *Biochem. Soc. Trans.* **2000**, *28*, 517–520.
- (49) *Cambridge Structural Database*, version 5.20; Cambridge Crystallographic Data Center, 12 Union Road, Cambridge CB2 1EZ, U.K.
- (50) MOLAC 7 (QCPE No. 688): Department of Chemistry, Indiana University, Bloomington, IN 47405.
- (51) Tetreault, S.; Ananthanarayanan, V. S. Interaction of calcium channel antagonists with calcium: structural studies on verapamil and its Ca²⁺ complex. *J. Med. Chem.* **1993**, *36*, 1017–1023.

JM020941H